

UC Riverside

UC Riverside Previously Published Works

Title

Aridity and plant uptake interact to make dryland soils hotspots for nitric oxide (NO) emissions

Permalink

<https://escholarship.org/uc/item/0xj6c45m>

Journal

Proceedings of the National Academy of Sciences of the United States of America, 113(19)

ISSN

0027-8424

Authors

Homyak, Peter M
Blankinship, Joseph C
Marchus, Kenneth
et al.

Publication Date

2016-05-10

DOI

10.1073/pnas.1520496113

Peer reviewed

Aridity and plant uptake interact to make dryland soils hotspots for nitric oxide (NO) emissions

Peter M. Homyak^{a,1,2}, Joseph C. Blankinship^a, Kenneth Marchus^a, Delores M. Lucero^b, James O. Sickman^b, and Joshua P. Schimel^a

^aEarth Research Institute and Department of Ecology, Evolution, and Marine Biology, University of California, Santa Barbara, CA 93106; and ^bDepartment of Environmental Sciences, University of California, Riverside, CA 92521

Edited by Donald E. Canfield, Institute of Biology and Nordic Center for Earth Evolution, University of Southern Denmark, Odense, Denmark, and approved March 23, 2016 (received for review October 15, 2015)

Nitric oxide (NO) is an important trace gas and regulator of atmospheric photochemistry. Theory suggests moist soils optimize NO emissions, whereas wet or dry soils constrain them. In drylands, however, NO emissions can be greatest in dry soils and when dry soils are rewet. To understand how aridity and vegetation interact to generate this pattern, we measured NO fluxes in a California grassland, where we manipulated vegetation cover and the length of the dry season and measured $[\delta^{15}\text{-N}]\text{NO}$ and $[\delta^{18}\text{-O}]\text{NO}$ following rewetting with ^{15}N -labeled substrates. Plant N uptake reduced NO emissions by limiting N availability. In the absence of plants, soil N pools increased and NO emissions more than doubled. In dry soils, NO-producing substrates concentrated in hydrologically disconnected microsites. Upon rewetting, these concentrated N pools underwent rapid abiotic reaction, producing large NO pulses. Biological processes did not substantially contribute to the initial NO pulse but governed NO emissions within 24 h postwetting. Plants acted as an N sink, limiting NO emissions under optimal soil moisture. When soils were dry, however, the shutdown in plant N uptake, along with the activation of chemical mechanisms and the resuscitation of soil microbial processes upon rewetting, governed N loss. Aridity and vegetation interact to maintain a leaky N cycle during periods when plant N uptake is low, and hydrologically disconnected soils favor both microbial and abiotic NO-producing mechanisms. Under increasing rates of atmospheric N deposition and intensifying droughts, NO gas evasion may become an increasingly important pathway for ecosystem N loss in drylands.

nitric oxide | chemodenitrification | drylands | NO pulses | N cycling

Nitric oxide (NO) is an important trace gas; it regulates the oxidative capacity of the atmosphere and indirectly influences Earth's climate (1). In the troposphere, NO catalyzes the production of hydroxyl radical, a powerful oxidant and cleanser of atmospheric contaminants. High concentrations of NO also favor the production of ozone (O_3), an urban pollutant and contributor to radiative forcing (1). Globally, fossil fuel combustion and biomass burning are major sources of NO, but soils are also a substantial source (2). Roughly 25–60% of terrestrial NO emissions originate from drylands (arid and semiarid environments) (3), which cover one-third of the terrestrial land surface (4), suggesting arid environments are important to global NO production. Climate models predict an expansion of drylands and intensifying droughts in existing arid regions (5), and when coupled with increasing rates of nitrogen (N) deposition and changes in the magnitude and frequency of precipitation events (6), increased soil NO emissions are possible (7). Paradoxically, arid soils are often described as infertile because biological processes are limited by water and N (8), raising the questions of why drylands are NO emission “hotspots.”

NO is produced in soils through both abiotic and biotic processes (2). Chemodenitrification encompasses all of the abiotic nonenzymatic processes that produce NO, including chemical decomposition of nitrous acid as well as reactions between N substrates with reduced metals and humic substances (9–11). The biological processes that produce NO, however, are numerous [e.g., nitrification, denitrification,

nitrifier denitrification, dissimilatory nitrate reduction to ammonium, and anaerobic ammonium oxidation (9)], but nitrification is generally considered the dominant driver of NO emissions under aerobic conditions (12). Nevertheless, both biotic and abiotic processes can occur simultaneously and are regulated by a range of environmental factors that complicate understanding of how NO emissions vary spatially and temporally.

At the soil-microsite scale, factors including pH, substrate supply, temperature, and, in particular, moisture, control the processes that produce NO (13, 14). Indeed, NO is frequently modeled as a function of water-filled pore space (WFPS), where NO emissions are highest when soils are moist and decline when soils are either drier or wetter than the optimum (14, 15); moist soils favor diffusion of resources to reaction sites while maintaining adequate gas diffusivity (16). In contrast, dry soils facilitate gas diffusion but limit substrate supply to reaction sites, whereas wet soils limit gas diffusivity and, therefore, NO emissions (17).

At the landscape scale, factors such as climate (aridity) and vegetation may influence environmental conditions in soil microsites and, therefore, may limit NO emissions even when optimal microsite-scale conditions are expected to favor NO production. In a chaparral ecosystem in southern California, NO emissions are not optimized when soils are moist during the wet season—emissions are in fact low (18). Rather, NO emissions are highest when soils are dry or when dry soils become wet following rewetting; similar patterns were observed in a tropical savannah in Venezuela (19) as well as in a desert floodplain in Arizona (United States) (20).

Significance

Nitric oxide (NO) controls the atmosphere's oxidative capacity. In soils, NO emissions are thought to be controlled by a tradeoff that develops in response to changes in soil moisture: dry soils limit substrate diffusion, whereas wet soils limit gas diffusivity, such that moist soils favor NO emissions. In drylands, however, NO emissions can be highest when soils are dry and immediately following rewetting. Aridity and vegetation interact to generate unexpected NO emission patterns. The shutdown in plant N uptake during the dry season causes NO emissions to increase, whereas arid conditions concentrate resources in dry soils, stimulating NO pulses upon rewetting. Chemistry governs the rapid initial NO pulse, whereas biological processes control later emissions as microbes recover from drought stress.

Author contributions: P.M.H., J.C.B., and J.P.S. designed research; P.M.H., J.C.B., K.M., and J.P.S. performed research; P.M.H., D.M.L., and J.O.S. contributed new reagents/analytic tools; P.M.H., J.C.B., K.M., D.M.L., J.O.S., and J.P.S. analyzed data; and P.M.H. wrote the paper with contributions from all authors.

The authors declare no conflict of interest.

This article is a PNAS Direct Submission.

¹Present address: Department of Ecology and Evolutionary Biology and Earth System Science, University of California, Irvine, CA 92697.

²To whom correspondence should be addressed. Email: phomyak@uci.edu.

This article contains supporting information online at www.pnas.org/lookup/suppl/doi:10.1073/pnas.1520496113/-DCSupplemental.

To understand the interactions among factors operating across scales and their effects on NO emissions, Firestone and Davidson developed a conceptual model using a “hole-in-the-pipe” metaphor (13). In their model, NO emissions are governed by the rate of N cycling (the diameter of the pipe), whereas factors such as soil moisture, pH, and temperature determine how much of that N may be transformed to NO (the holes). In this sense, aridity and vegetation may offset the balance of importance in microsite-scale controls (e.g., moisture, temperature, and substrate supply), influencing both the rate of N flowing through the pipe and the side reactions that produce NO. For example, plants are fierce competitors for N (21, 22) and, through root uptake, may limit N availability and, therefore, N supply for NO production. In both the chaparral and tropical savannah, moist conditions occurred during the plant growing season, raising the possibility that plants could constrain N availability, thereby limiting NO emissions (18, 19). Aridity, on the other hand, may influence NO emissions by favoring NO-producing mechanisms when dry soils are rewet (23–25). In drylands, asynchrony between N availability and plant demand (26) and between soil C mineralization and nitrification (27) limit N retention and could cause drylands to operate as NO hotspots.

Building on the hole-in-the-pipe conceptual model, we explore the possibility that vegetation and aridity can influence microscale controls, generating NO emission patterns opposite to those observed in laboratory incubation studies. To develop our arguments we ask: (i) Can plants influence seasonal NO emission patterns in the field? (ii) How do arid conditions favor NO emissions? (iii) How does the balance between biotic and abiotic processes control NO pulses upon rewetting dry soils?

We used a semiarid grassland to understand how plant N uptake and aridity, and interactions between them, influenced NO emission patterns. To isolate the effects of vegetation, we created four levels of plant removal (0%, 30%, 60%, and 90% thinning). Effects of aridity were assessed by manipulating the length of the dry season through a combination of irrigation and rainfall exclusion treatments; we studied NO emissions in “Ambient,” “Extended dry season,” “Short dry season,” and “No dry season” plots. We measured soil N pools to understand how interactions between aridity and vegetation influenced available N for NO production. We also used an isotope tracer approach in the field to measure $[\delta^{15}\text{-N}]\text{NO}$ and $[\delta^{18}\text{-O}]\text{NO}$ isotope fluxes using passive collectors (NO_x pads; Ogawa & Co.). The $[\delta^{15}\text{-N}]\text{NO}$ and $[\delta^{18}\text{-O}]\text{NO}$ measurements were used to distinguish between biotic and abiotic NO-producing mechanisms and to understand what forms of N generated NO upon rewetting. Specifically, $[\delta^{18}\text{-O}]\text{NO}$ measurements used the naturally occurring evaporation-induced fractionation of oxygens in soil water to determine whether substrates synthesized during the antecedent dry season produced NO pulses. We hypothesized (i) that drylands act as NO emission hotspots because interactions between aridity and vegetation maintain a “leaky” N cycle and (ii) that periods of high NO flux are governed by a shutdown in plant N uptake and by arid conditions that stimulate NO-producing abiotic and biotic mechanisms.

Results

Vegetation Controls on Soil NO Emissions. Removing plants increased NO fluxes (Fig. 1). Regardless of dry season length, average NO emissions across all plots were lower with plants ($3 \text{ ng N m}^{-2} \text{ s}^{-1}$) than after 90% thinning ($7 \text{ ng N m}^{-2} \text{ s}^{-1}$) (hereafter, denoted “without plants”); 30% thinning increased NO emissions by 23% ($P = 0.2$), 60% thinning increased NO emissions by 45% ($P = 0.003$), and removing plants more than doubled NO flux rates ($P < 0.0001$), but these differences were greatest in the plots that received the least summer water. Because NO emissions increased with increasing plant removal, we focus our discussion on the effects of 90% thinning to better understand how vegetation influences soil NO emissions (Fig. 1).

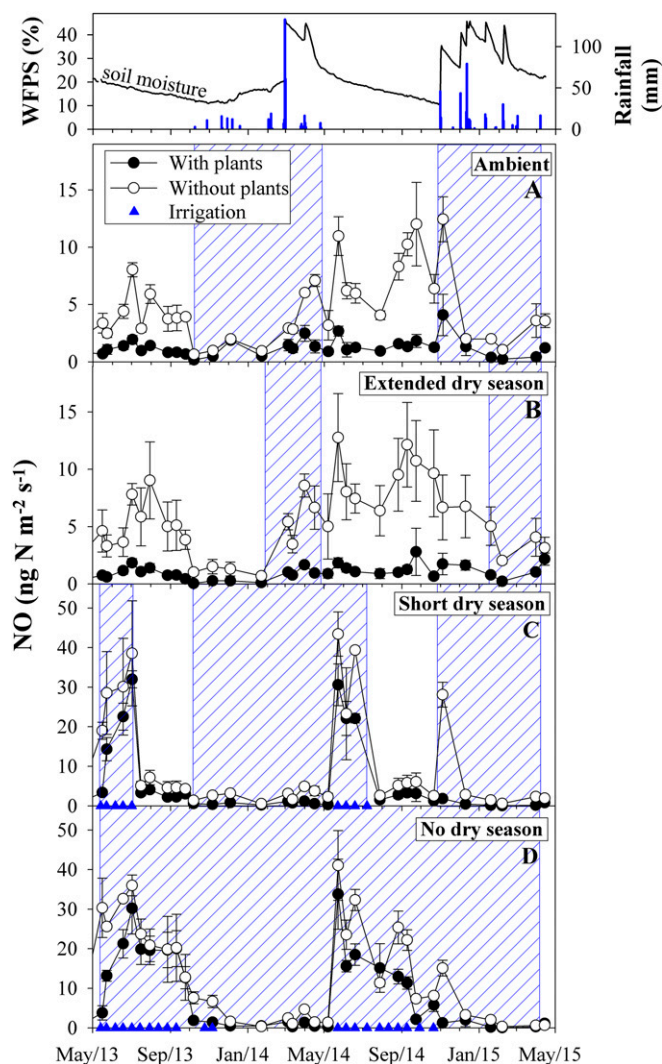


Fig. 1. (Lower) Average (\pm SEM; $n = 3$) soil NO fluxes from plots with and without plants under Ambient conditions (A), Extended dry season (B), Short dry season (C), and No dry season (D). Irrigation periods are represented by triangles on the x axis of the Short dry season and No dry season treatments. Hashed boxes represent the wet season, as controlled by natural rainfall (A), rainfall exclusion shelters (B), or combined irrigation with rainfall (C and D). (Upper) Soil WFPS and rainfall measured at the nearby Lisque weather station.

In the Extended dry season treatment, removing plants increased NO emissions by $\sim 5.5\times$ ($P < 0.0001$), whereas in the Ambient plots, plant removal increased fluxes by $\sim 4\times$ ($P = 0.0025$; Fig. 1A). In contrast, irrigating soils reduced the effects of plant thinning; in the Short dry season, removing plants increased NO emissions by $1.8\times$ ($P = 0.03$), whereas in the No dry season plots, removing plants increased emissions by $1.6\times$ ($P = 0.02$; Fig. 1 C and D).

Effects of Dry Season Length on NO Emissions. In Ambient plots with plants, average NO emissions during the dry season were $\sim 3\times$ higher ($1.2 \text{ ng N m}^{-2} \text{ s}^{-1}$) than during the wet season ($0.5 \text{ ng N m}^{-2} \text{ s}^{-1}$; $P < 0.0001$; Fig. 1A) when we excluded fluxes measured within 4 d of natural precipitation (i.e., NO emissions generated during a rewetting pulse). Similar patterns occurred in Ambient plots without plants, where dry season NO emissions averaged $5.6 \text{ ng N m}^{-2} \text{ s}^{-1}$ and were greater than during the wet season ($1.7 \text{ ng N m}^{-2} \text{ s}^{-1}$; $P < 0.0001$; Fig. 1A).

Dry season length had varying effects on soil NO emissions. Whereas extending the length of the dry season did not affect NO

emissions compared with Ambient plots ($P = 0.97$), irrigating soils in the Short dry season increased average NO emission rates by 2.6× above Ambient plots ($P < 0.0001$) and nearly quadrupled the overall fluxes in the No dry season plots (Fig. 1 C and D; $P < 0.0001$). NO emission rates returned to background rates when irrigation ended in July (Fig. 1C).

NO Pulses. Rewetting soils at the end of the dry season (September to October) produced NO emission pulses up to 9× greater than prewetting emissions rates within 30 s of adding water (“prewetting” vs. “wetting”; Fig. 2). In general, emission rates during these pulses peaked within 24 h postwetting, decreasing to rates similar to prewetting conditions within 2–4 d (Fig. 2).

Plants also governed the magnitude of NO pulses during rewetting. On average across all plots, NO pulses were 1.4× higher without plants than with plants (Fig. 2; $P = 0.02$). Manipulating the length of the dry season had varying effects. Extending the length of the dry season appeared to reduce NO pulses by 49% below Ambient plots (Fig. 1B; $P < 0.0001$). However, after correcting for the temperature difference between September to October and January using a temperature correction coefficient (Q_{10}) of 2 (2)—Extended dry season plots were rewet during winter after removing the rainout shelters—there was no longer a significant effect ($P = 0.25$). Shortening the length of the dry season had no effect on NO pulses when comparing Short dry season to Ambient plots (Fig. 2C; $P = 0.94$), but in the No dry season plots, maintaining moist soils lowered NO pulses by 33% compared with Ambient plots (Fig. 2D; $P = 0.009$).

Soil N Dynamics. In Ambient plots with plants, total extractable N (TEN) (which includes both organic and inorganic forms) trended upward as soils dried during 2013 (May to September; Fig. 3A; $P = 0.08$) and 2014 (May to October; Fig. 3A; $P = 0.002$); the trend was driven by water-extractable organic nitrogen (WEON) increasing by $\sim 3 \mu\text{g g}^{-1}$ in 2013 and by $11 \mu\text{g g}^{-1}$ in 2014, whereas NH_4^+ and NO_3^- remained relatively unchanged (Fig. 3A). The most substantial change in NH_4^+ and NO_3^- occurred at the onset of the wet season (December 2014), when NH_4^+ concentrations decreased by 65% and NO_3^- concentrations tripled (October 2014; Fig. 3A). Without plants, Ambient TEN also increased as soils dried out in 2013 (May to September; Fig. 3A; $P = 0.04$), but in contrast to plots with plants, increases in both NH_4^+ and NO_3^- contributed to the upward trend (Fig. 3A). During the 2014 dry season, however, although TEN concentrations remained high, a significant temporal trend was not detected (May to October; Fig. 3A; $P = 0.9$).

Overall, TEN, WEON, NO_3^- , and NH_4^+ were higher without plants than with plants (Fig. 3; $P < 0.0001$), whereas manipulating the length of the dry season had varying effects. Extending the length of the dry season increased NH_4^+ by 28% above Ambient plots ($P = 0.02$), decreased NO_3^- by 29% ($P = 0.01$), and had no effect on WEON ($P = 0.9$) or TEN ($P = 0.8$) (Fig. 3B). Shortening the length of the dry season increased NO_3^- by 58% above Ambient plots ($P = 0.01$) and by 38% when we kept soils consistently moist (No dry season plots; $P = 0.002$). In contrast, WEON decreased by 29% below ambient plots in the Short dry season plots ($P = 0.002$) and by 45% in the No dry season plots ($P = 0.001$). Irrigating soils did not have a significant effect on NH_4^+ or TEN concentrations ($P > 0.3$) (Fig. 3 C and D).

TEN increased during summer 2013 in the No dry season plots (May to September) with or without plants ($P < 0.01$; Fig. 3D). In these moist soils, increases in TEN during the 2013 dry season were driven by the buildup of NO_3^- and NH_4^+ as WEON decreased in September (Fig. 3D). During summer 2014, TEN also generally increased in plots with plants (May to October; Fig. 3D; $P = 0.14$), but in plots without plants, the upward trend weakened ($P = 0.6$); WEON, NO_3^- , and NH_4^+ remained relatively high and varied little (Fig. 3D).

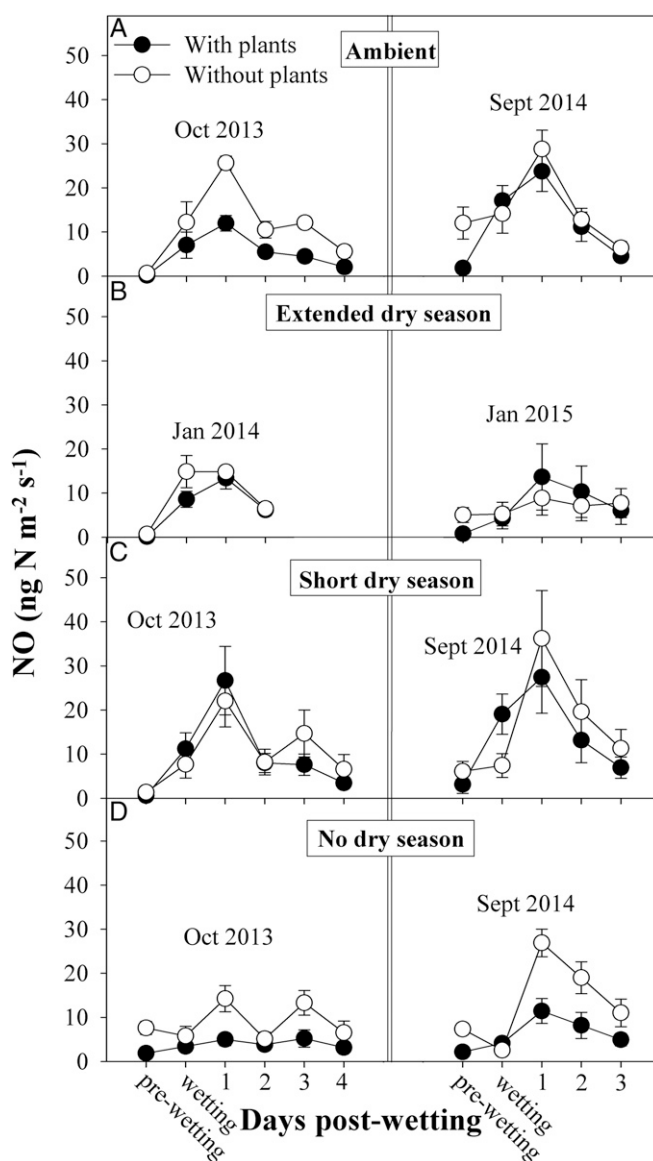


Fig. 2. Average (\pm SEM; $n = 3$) soil NO fluxes during pulses generated after rewetting dry soils in plots with and without plants under Ambient conditions (A), Extended dry season (B), Short dry season (C), and No dry season (D). Rewetting experiments were made during October 2013 and September 2014 in Ambient, Short dry season, and No dry season plots. Extended dry season plots were rewetted in January 2014 and 2015, when rainout shelters were removed. Because of cooler temperatures in January, we corrected NO fluxes using a Q_{10} of 2 (2). Correcting for temperature produces NO pulses indistinguishable from Ambient plots ($P = 0.25$).

Soil NO_2^- concentrations averaged $0.6 \mu\text{g N g}^{-1}$ and made up to 4% of the TEN (Fig. 3). In general, thinning or dry season length did not significantly affect NO_2^- concentrations (Fig. 3; $P > 0.33$), although on average, maintaining soils consistently moist in the No dry season plots lowered NO_2^- by 27% compared with Ambient plots. Over the length of the dry season, NO_2^- concentrations trended upward as the number of days without rainfall increased, but the upward trends were not significant in either 2013 ($P = 0.58$) or 2014 ($P = 0.32$) (Fig. S1).

In Ambient plots with plants, net N mineralization averaged $0.03 \mu\text{g N g}^{-1} \text{d}^{-1}$ and net nitrification $0.06 \mu\text{g N g}^{-1} \text{d}^{-1}$ without varying substantially over time ($P > 0.9$; Fig. S1). Similarly, averaged across time, we did not detect a significant effect of plant thinning

efflux (31). However, we found that NO emissions decreased when soils were moist, while increasing in dry soils and during short periods following abrupt rewetting events. Here, we explore how vegetation and aridity interact to generate patterns opposite to those expected from laboratory studies by (i) maintaining an open N cycle (N loss vs. N recycled) during periods when plant N uptake is low and by (ii) favoring both biotic and abiotic NO-producing reactions.

Removing plants increased soil N availability, such that the N otherwise used by plants could have been used by microbial processes that produce NO. Although removing plants did not significantly increase rates of nitrification, on average, these rates were 10–20× higher in the absence of plants during both the dry-to-wet transition and spring (Fig. S2). Similar patterns were observed in an earlier study at our site, where N mineralization and nitrification rates and nitrification potentials—an index of nitrifier populations—significantly increased during summer, when plants senesced (32). According to the hole-in-the-pipe model, a higher N flux would

produce a larger pipe, therefore resulting in higher NO emissions in the absence of plants. Based on these effects, we expected plant phenology would help explain seasonal NO emission patterns at our site [i.e., explain why NO emissions increased as soils dried and plants senesced, similar to observations in another dryland study (18)]. In support of plants controlling NO emissions, differences in plant species composition explained differences in NO flux between two forested sites (33), whereas other studies have suggested that plant N uptake controls hydrologic N loss (26, 34) and, therefore, plants should also be capable of influencing gaseous N export (2, 18, 26). Thus, during the dry season, NO emissions likely increased because the shutdown in plant N uptake increased N supply to NO-producing processes and reactions.

In drying soils, products from nitrification can increase N availability in the absence of plant uptake (Fig. 3), potentially favoring N loss via gaseous pathways. Although nitrifiers are sensitive to drought (35), they can remain active in thin water films formed as soils dry (23, 36), possibly explaining how interactions between vegetation and aridity caused NO emissions to increase during summer. In these diffusion-limited environments, the accumulation of microbial metabolic products (e.g., NH_4^+ , NO_2^- , and NO_3^-) may maintain a flux of NO even as soils dry (23, 26, 32, 37). NO_2^- , in particular, is chemically reactive (38) and, in dry soils, may be less likely to be oxidized by nitrifiers but may still chemodenitrify (10, 29, 39). At our site, NO_2^- concentrations averaged $0.6 \mu\text{g NO}_2^- \cdot \text{N g}^{-1}$ (Fig. S1). Assuming a sustained dry season flux of $5 \text{ ng NO-N m}^{-2} \text{ s}^{-1}$, the NO_2^- pool in surface soils (top 5 cm) could in principle generate NO for roughly 10 mo. In the competition between biology and chemistry, dry soils may favor abiotic over biotic processes, producing NO via abiotic NO_2^- decomposition.

Besides the decoupling between plant N uptake and soil N cycling during the dry season, rewetting soils also produced conditions where cooccurring biotic and abiotic processes governed NO efflux. During pulses generated upon rewetting soils, NO emissions were driven by the mixing of a (i) “reactive” NO source, predominantly abiotic, producing NO within 15 min postwetting with a (ii) slower-to-react, but “emergent,” biological source stimulated by the oxidation of NH_4^+ , presumably as ammonia-oxidizing bacteria (AOB) or archaea recovered from drought-induced stress. This supposition is strongly supported by the isotope-tracer experiments, which showed that labeled NO_2^- was immediately converted into NO, whereas it took several hours for conversion of labeled NH_4^+ into NO.

The reactive NO source was controlled by the cooccurrence of abiotic and biotic processes sustained by the consumption of NO_2^- and NO_3^- . In support of abiotic transformations of NO_2^- to NO (chemodenitrification), NO emissions increased by roughly an order of magnitude within 30 s of rewetting soils, and such dramatic and rapid increase is inconsistent with biological process, which require 10s of minutes to recover from drought-induced stress (40, 41). NO_2^- -oxidizing bacteria are also slower to recover from stress than AOB (42), and because $^{15}\text{N}[\text{NH}_4^+]$ -labeled substrates did not generate appreciable NO until after 15 min postwetting (Fig. 4A), it is unlikely that NO_2^- was biologically converted into NO. In contrast, assuming a sustained flux of $30 \text{ ng NO-N m}^{-2} \text{ s}^{-1}$, equivalent to the peak NO flux we measured during a rewetting pulse, the NO_2^- pool made available by the rewetting event, alone, could generate NO for 4 d via chemodenitrification.

The production of NO via chemodenitrification is also supported by our $[\delta\text{-}^{15}\text{N}]\text{NO}$ and $[\delta\text{-}^{18}\text{O}]\text{NO}$ measurements. First, the $^{15}\text{N}[\text{NO}_2^-]$ label peaked during the first 15 min postwetting, well above the signals generated by either $^{15}\text{N}[\text{NO}_3^-]$ or $^{15}\text{N}[\text{NH}_4^+]$ (Fig. 4A), suggesting NO emitted during this time period was almost exclusively derived from NO_2^- . Second, the NO produced during the first 15 min postwetting was enriched in ^{18}O relative to other time periods (Fig. 4B), indicating the NO_2^- used to produce NO during the first 15 min postwetting must have been synthesized during the antecedent dry season and not by microbes resuscitated by the rewetting pulse. Because evaporation fractionates the isotopic

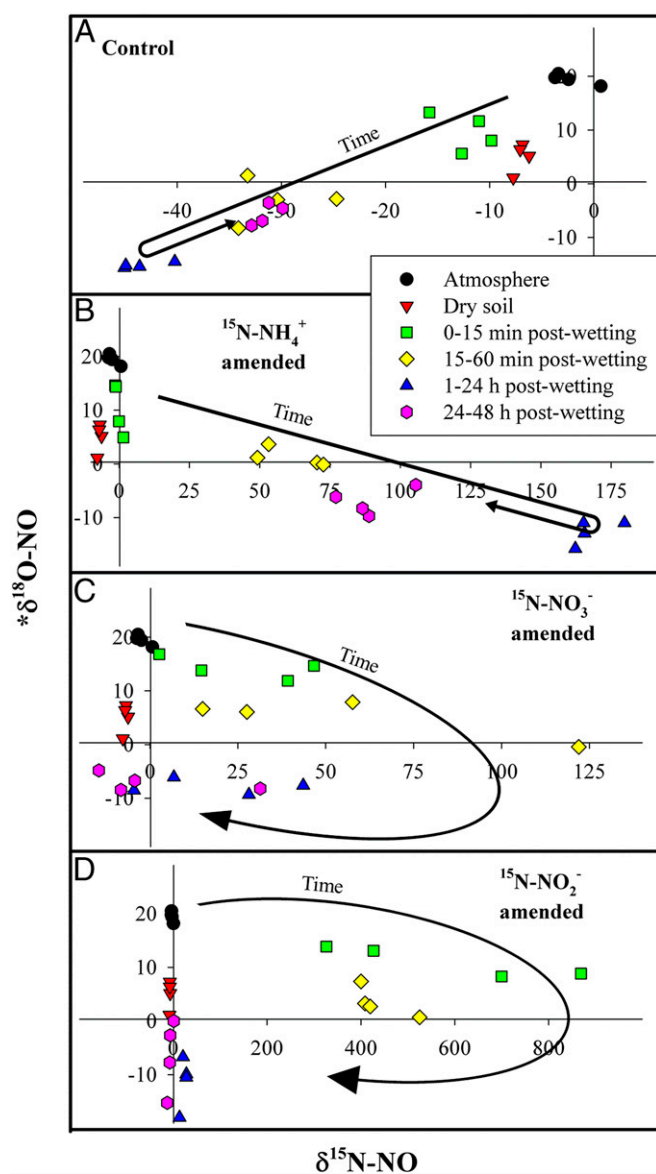


Fig. 5. Dual isotope plot ($[\delta\text{-}^{15}\text{N}]\text{NO}$ and $[\delta\text{-}^{18}\text{O}]\text{NO}$) following the rewetting of dry soils in September 2014. Soils rewetted with 500 mL of DIW are denoted controls (A), whereas other soils were rewetted with 500-mL solutions containing 1 atom% $^{15}\text{N}[\text{NH}_4^+]$ (B), $^{15}\text{N}[\text{NO}_3^-]$ (C), and $^{15}\text{N}[\text{NO}_2^-]$ (D).

composition of water (43), the soil solution becomes enriched in ^{18}O through evaporation. In contrast, during the peak flux postwetting (1–24 h), the $[\delta^{18}\text{O}]\text{NO}$ approached the $\delta^{18}\text{O}$ of the rewetting solution (-17% ; Fig. 4B), suggesting that the substrates used to generate NO were synthesized in situ, consistent with the time required by nitrifiers to recover from drought stress (42). Thus, at the onset of the rainy season, rewetting soils favors chemodenitrification, representing an important pathway whereby NO_2^- is chemically decomposed to NO.

Besides chemodenitrification, denitrification may have contributed to the reactive NO source, albeit to a lesser extent. Within 15 min of adding the $[\text{N}^{15}]\text{NO}_3^-$ tracer, the ^{15}N label started to appear in NO but peaked during the interval 15–60 min postwetting (Fig. 4A). This rapid incorporation of $[\text{N}^{15}]\text{NO}_3^-$ into NO was surprising—drylands are not considered denitrification hotspots, and we added a relatively small amount of water to very dry soils—but this rapid incorporation is not inconceivable. At our site, denitrification potentials and denitrifying enzyme activity increase in step with microbial biomass as soils dry (32), perhaps suggesting denitrifiers may be capable of processing NO_3^- within 15 min of rewetting soils.

In contrast to the reactive NO source, the emergent and slower to react NO source was driven by the relatively less rapid oxidation of NH_4^+ by AOB or archaea, which controlled the peak NO flux 1–24 h postwetting while fractionating $\delta^{15}\text{N}$ by 31‰. We hypothesize that NH_4^+ was not only derived from pools concentrated over the summer but also from mineralization of a light-fraction organic N pool released upon rewetting (44) that, in our case, may be represented by the WEON pool. WEON decreased in step with irrigation frequency producing smaller NO pulses upon rewetting dry soils at the onset of the wet season. In support of NH_4^+ oxidation, we observed high NO_3^- concentrations and nitrification rates upon rewetting soils—a pattern observed in our study site and other drylands (26, 32)—and note that a 31‰ $\delta^{15}\text{N}$ fractionation effect is consistent with nitrification (32, 45). Although we cannot conclusively differentiate between nitrification or nitrifier denitrification as the source of NO, nitrifier denitrification can account for a substantial fraction of NO emissions (11, 46) and may best explain the $[\delta^{18}\text{O}]\text{NO}$ isotopic trends we observed.

During nitrification, NO is derived from hydroxylamine (NH_2OH) (9), where the O is derived from air (47). In contrast, during nitrifier denitrification NO is derived from the reduction of NO_2^- by nitrifiers (9), where one of the oxygens in NO_2^- is derived from air and the other from water (47, 48). During our measurements, the peak consumption of NH_4^+ coincided with the lowest $[\delta^{18}\text{O}]\text{NO}$, resembling the $\delta^{18}\text{O}$ composition of the rewetting solutions. This shift in $\delta^{18}\text{O}$, from +10‰ to -15% $\delta^{18}\text{O}$, suggests that the peak NO flux was derived from NO_2^- generated in situ as a consequence of the rewetting pulse and, hence, by nitrifier denitrification upon the recovery of nitrifiers from drought-induced stress—NO derived from nitrification should have been insensitive to the $\delta^{18}\text{O}$ composition of the added water. These interpretations support the understanding that nitrifier denitrification is an important mechanism for microbes to avoid accumulating toxic levels of NO_2^- (49), perhaps in response to the NO_2^- flush generated upon rewetting dry soils.

In this context, the emergent source represents an acceleration in nitrifier activity during the recovery from drought-induced stress, which gradually controlled the $[\delta^{15}\text{N}]\text{NO}$ signal 1–24 h postwetting. Thereafter, as biological processes slowed, $[\delta^{15}\text{N}]\text{NO}$ trended back, along the mixing line between biotic and abiotic processes, toward the signal of the reactive NO source—a source that, in principle, we estimated can generate NO for at least 4 d postwetting—suggesting that chemodenitrification may contribute to NO emissions when soils are dry. Consistent with this understanding, we also observed a linear trend when soils were rewet with $[\text{N}^{15}]\text{NH}_4^+$ generating a mixing line that mirrored the DIW-generated line but in the direction of the added tracer (Fig. 5B). These patterns confirm that NH_4^+ oxidation operated as an endmember (i.e., the emergent source) driving the isotopic composition of NO toward -43% $\delta^{15}\text{N}$

(Fig. 5A). In contrast, the “clockwise” hysteresis observed with $[\text{N}^{15}]\text{NO}_2^-$ and $[\text{N}^{15}]\text{NO}_3^-$ tracers (Fig. 5C and D) suggests that although NO produced by chemodenitrification and denitrification governed the initial NO pulse, these processes were overwhelmed by the oxidation of native soil NH_4^+ made available upon rewetting soils in the field. This strongly fractionating signal “pulled” the $[\delta^{15}\text{N}]\text{NO}$ toward -43% $\delta^{15}\text{N}$, thereby generating the clockwise hysteresis. These conclusions are supported by the more than doubling rate in NO emitted 24 h postwetting compared with that emitted immediately postwetting (Fig. 2A), which coincides with the period when NH_4^+ oxidation dominates NO emissions.

At the landscape scale, these interactions between aridity and vegetation are important because the interactions can influence the trajectory of ecosystem N cycling (50); that is, whether N is exported or internally cycled. For example, arid soils tend to be ^{15}N -enriched, whereas soils in temperate mesic systems tend to be ^{15}N -depleted (51), suggesting an N cycle that is more open (N loss vs. N recycled) is inherent to the mechanisms governing N cycling in arid landscapes (8, 50, 51). Because aridity controls vegetation and water availability (52), N cycling in arid systems is less influenced by plants and more so controlled by interactions between microbial and abiotic processes (51). Building on this understanding, it is thought that in arid systems, microbial processes controlling N gas evasion may regulate the fate of soil $\delta^{15}\text{N}$ (51), because these emissions can represent a substantial fraction of ecosystem N loss (18, 26), while strongly discriminating against ^{15}N (45). Leaching of NO_3^- to subsoils or groundwater can also produce ^{15}N -rich surface soils (53), although leaching is less important in arid regions and less fractionating than gaseous processes (51). Our measurements suggest that NO emissions, especially those generated by nitrification, significantly contribute to the openness of arid ecosystems and to the enrichment of soil $\delta^{15}\text{N}$ during “hot moments” controlled by rapid shifts from dry-to-wet soil conditions.

Conclusions

Our measurements suggest that ecosystem NO emissions increase when plant N uptake and soil N cycling decouple during the dry season, increasing N supply to NO-producing biotic and abiotic processes in soils. At the onset of the wet season, rewetting soils generate NO pulses via chemodenitrification, whereby NO_2^- generated during the antecedent dry season abiotically decomposes to NO. Over time, microbial processes recover from drought stress and regain control of NO production, while reducing the magnitude of NO pulses generated upon rewetting soils. These mechanisms suggest that drylands are well equipped to convert N into NO and that under increasing rates of atmospheric N deposition and changes in climate favoring droughts (5), NO gas evasion may become an increasingly important pathway for ecosystem N loss in arid and semiarid regions.

We conclude that aridity and vegetation may operate as “ultimate” controls, those capable of transforming ecosystems (54, 55) by governing spatial and temporal patterns in N uptake and availability. Under the influence of these controls, drylands or regions experiencing pronounced shifts from dry-to-wet soil conditions may operate as NO hotspots because interactions between aridity and vegetation maintain a leaky N cycle during periods when plant N uptake is low, and hydrologically disconnected soils favor both microbial and abiotic NO-producing mechanisms.

Materials and Methods

Site Description. We studied a seasonally dry grassland at the University of California Sedgwick Reserve near Santa Barbara, CA [370 m above sea level (ASL); 34.7120 N, 120.0388 W]. The vegetation at our site is dominated by nonnative Mediterranean annual grasses—primarily *Bromus diandrus*, *Bromus hordeaceus*, and *Avena fatua*. The climate is Mediterranean with hot dry summers and cool wet winters (Fig. S3A). The mean annual precipitation is 380 mm, with an average annual temperature of 16.8 °C: daytime air temperatures average 33 °C in summer and rarely drop below 0 °C during winter nights. Roughly 90% of annual precipitation falls between November and April. The water year (WY) officially begins on October 1 and ends on

September 30. During the 2 y of the study, annual precipitation was roughly 50% below average (175 mm in WY 2013 and 201 mm in WY 2014). Soils are described as Pachic Haploxerolls with silty clay loam texture and granular structure on nearly flat slopes (<2%) and derived from the Paso-Robles formation consisting of poorly consolidated alluvial material formed from montmorillonite that eroded from nearby Monterey Shale deposits. The soils are rich in 2:1 clays and also contain some amount of Franciscan Complex minerals including ultramafics (e.g., serpentinite), sandstone, and chert. The soil pH is 6.9, with 2.2% C, 0.21% N, and a bulk density of 1.2 g cm⁻³ in the upper 10 cm.

Vegetation and Dry Season Length Manipulations. To quantify the effect of vegetation and dry season length on NO emissions, we maintained plots (2 m × 1 m) for 2 y with four levels of plant removal (0%, 30%, 60%, and 90% plant thinning) and four levels of dry season length (Ambient, Extended dry season, Short dry season, and No dry season).

Our experimental plots were selected in December 2012 based on similar plant cover and composition; plots were segregated into three blocks, each block containing 16 plots (four levels of vegetation × four levels of dry season length), for a total of 48 plots ($n = 3$ for each treatment). We oriented all plots with the longer 2-m side spanning from north to south and spaced at least 1 m apart to minimize edge effects. Thinned plots were maintained every 7–10 d during the growing season and as needed during the dry season. Edge effects of root growth from outside the plots were minimized by clearing a ~30-cm perimeter around every plot using a motorized weed trimmer.

The unthinned plots (0% thinning; denoted “with plants”) were not altered. In plots thinned by 30% or 60%, roughly one-third or two-thirds of the above-ground biomass was evenly pulled out by hand while minimizing soil disturbance. In the 90% thinning plots (without plants), we removed all plants, but because of germination between site visits, we refrain from referring to the treatment as “100% thinning.” Thinning occurred through the end of WY 2014. Averaged across two years, 90% thinning increased soil moisture by 5% in Ambient plots.

The Ambient treatments represented field conditions—in California the dry season typically lasts 6 mo (from May until October; Fig. S3A).

The Extended dry season delayed rainfall until January (i.e., ~9 mo) using rainout shelters that kept soils dry. Rainout shelters (2.5 m × 1.2 m) used in Extended dry season plots were built from clear corrugated polycarbonate roof panels (Suntuf; Palram Americas) attached to a metal frame. We did not observe any consistent effect of the shelter on soil temperature (e.g., greenhouse effect) or soil moisture (e.g., dew accumulation). To extend the WY 2013 dry season, shelters were in place from October 7, 2013 until January 30, 2014 and from October 24, 2014 until January 19, 2015 for WY 2014 (Fig. S3B).

The No dry season treatment was designed to maintain soils consistently moist during the typical 6-mo dry season (32). The Short dry season was similar to the No dry season, except that soils were irrigated and kept consistently moist for only about half of the dry season. Thereafter, soils were allowed to dry until rewet by rainfall. No dry season plots were irrigated 12 times in the 2013 dry season (May 14 through November 6; 180 mm total water added) and 10 times in the 2014 dry season (May 23 through October 21; 150 mm total water added; Fig. S3B), roughly equivalent to adding 3 kg N ha⁻¹ yr⁻¹. Short dry season plots were irrigated five times in the 2013 dry season (May 14 through July 2; 75 mm total water added) and four times in the 2014 dry season (May 23 through July 8; 60 mm total water added; Fig. S3B), roughly equivalent to adding 1.5 kg N ha⁻¹ yr⁻¹. The background atmospheric N deposition rate at Sedgwick is ~5–7 kg N ha⁻¹ yr⁻¹ (56).

The predetermined threshold between “moist” and “dry” soil was 10% volumetric water content (VWC) or 18% WFPS. Soil WFPS was defined as

$$\text{WFPS} = \frac{\text{VWC}}{1 - \left(\frac{\rho_b}{\rho_s}\right)}, \quad [1]$$

where VWC is soil volumetric water content, ρ_b is the bulk density (1.2 g cm⁻³), and ρ_s is the particle density (2.65 g cm⁻³). In these soils, a marked decline in respiration occurs below 18% WFPS (57), suggesting that microbes rapidly lose access to C substrates as soils dry below this threshold. Therefore, we irrigated as soon as soils dried to 18% WFPS in the spring (when soils begin to dry) and continued irrigating until the first rain event in the fall (the onset of the wet season) for the No dry season or until July for the Short dry season.

Each irrigation event consisted of adding 30 L (equivalent to 1.5 cm of rainfall) of local well water [0.003 mg NH₄⁺-N L⁻¹, 1.6 mg NO₃⁻-N L⁻¹, 0.4 mg dissolved organic nitrogen (DON) L⁻¹] to each plot every 2–3 wk. Plots were irrigated using a backpack sprayer with a fine nozzle to minimize soil disturbance. Because of the sprayer’s 15-L capacity and the desire to allow time for infiltration, the 30 L of water was added in two 15-L “doses” spaced roughly 1 h apart. Based on field measurements of soil moisture using a portable MiniTrase Time Domain Reflectometer (Soil Moisture Equipment Corporation), each irrigation

event moistened soils in the top 10 cm to ~50% WFPS. Then, on average, soils dried by 2% WFPS per day, particularly during the middle of the summer. Thus, irrigation was required every 2 wk to prevent drying below 18% WFPS.

Based on a soil porosity of 54% ($1 - \rho_b/\rho_s$), we expected the irrigation water to infiltrate at least 3 cm, wetting 66 kg of soil in No dry and Short dry season plots. Under these conditions, and assuming steady state, irrigating soils for two dry seasons would have raised the N content of soils to 0.03 μg NH₄⁺-N g⁻¹, 16 μg NO₃⁻-N g⁻¹, and 4 μg organic N g⁻¹ in the No dry season plots. For the Short dry season watering roughly raised the N content of soils over 2 y to 0.01 μg NH₄⁺-N g⁻¹, 7 μg NO₃⁻-N g⁻¹, and 2 μg organic N g⁻¹.

NO Emission Measurements. Three months before measuring NO emissions, a polyvinylchloride collar (PVC) (30.5-cm diameter × 10-cm height) was inserted 6 cm into the ground at each of the 48 plots under vegetation and dry season length manipulations. The placement of collars did not impede the growth of plants.

Rates of soil NO emissions were measured by soil chamber methodology (58) using a Scintrex LMA-3 chemiluminescent NO₂ analyzer. The flux of NO was calculated based on the physical dimensions of the chamber, the rate of change in NO concentrations inside the chamber, and air temperature:

$$F = \frac{dC}{dt} \times \frac{VN}{ART} \quad [2]$$

where F is the NO flux rate (ng NO-N m⁻² s⁻¹); dC/dt [parts per billion by volume (ppbv) NO-N s⁻¹] is the rate of NO concentration increase inside the chamber computed by linear regression; V is the chamber volume (L); N is the atomic weight of nitrogen (14.01 g mol⁻¹); A is the area of the PVC collar (730 cm²); R is the gas constant (0.0821 L atm mol⁻¹ K⁻¹); and T is the chamber air temperature (K). NO emissions were measured approximately every 2–4 wk from May 8, 2013 to April 14, 2015. During the dry season, NO emissions were measured biweekly, within 3–5 h of irrigating soils.

Rates of soil trace gas emissions were determined by placing a PVC chamber (volume, 11 L), equipped with a small fan (4-cm diameter), over the previously installed PVC collars and measuring the change in concentration of NO inside the chamber headspace for ~3–6 min. During measurements, chamber air flowed into the analyzer and makeup ambient air flowed into the chamber through a vent. Because the LMA-3 analyzer only measures the concentration of NO₂, a CrO₃ in-line oxidizer (Drummond Technology) was placed in line to convert NO into NO₂. During sampling, NO₂ did not accumulate in the chambers, suggesting that increases in the instrument signal were attributable entirely to NO. A Nafion tube drier (Perma Pure DM-110-24) was used to remove moisture from the chamber air before entering the CrO₃ oxidizer, because humidity can limit the conversion of NO to NO₂ (59). Although we did not measure O₃ directly, at NO₂ mixing ratios <1 ppb, 1 ppb of O₃ can induce a 0.003-ppb increase in the instrument signal (60). Annual concentrations in Santa Ynez, ~9 km south from our site, averaged 4 ppb NO₂ and 57 ppb O₃ in 2013 (61), suggesting negligible impact of O₃ on our measurements. The LMA-3 was calibrated in the field before and after each series of NO measurements. For calibration purposes, a standard curve was made by mixing an NO standard (0.0988 ppmv NO in N₂ gas; Scott-Marrin) with zero-grade air. The method detection limit was 0.02 ppbv NO.

In October 2013 and September 2014, we added 500 mL of DIW to the soils inside PVC collars, except for soils in the extended dry season treatments, which were rewetted in January 2014 and 2015 after removing the rain shelters.

Rewetting and Isotope Tracer Experiments. To characterize how plants and dry season length influenced the magnitude and duration of NO pulses, we monitored NO emissions after rewetting soils in the late dry season. In October 2013 and September 2014, we added 500 mL of DIW to the soils inside PVC collars, except for soils in the extended dry season treatments, which were rewetted in January 2014 and 2015 after removing the rain shelters. NO emissions were measured the moment before adding water to characterize prewetting emissions, immediately after adding water (within 20 s; wetting) to characterize the initial NO pulse, and 1–4 d postwetting to characterize the peak of the NO pulse, as well as the duration of the pulse—the “trail-off” period when NO emissions trended toward prewetting conditions.

To understand the mechanisms controlling NO emissions during the wetting, peak, and trail-off periods, we measured [δ-¹⁸O]NO and [δ-¹⁵N]NO emitted from soils. In September 2014, we established five new plots (3 m × 3 m) and installed 4 chambers (300-cm² surface area) in each of the five plots, for a total of 20 chambers. In one of the plots, four chambers were used to measure ambient conditions and capture the isotopic signature of NO emitted from dry soils. Another set of chambers, in a second plot, served as a controls ($n = 4$), where the soils inside the chambers were rewetted with 500 mL of DIW (1.7 cm). The chambers in the remaining three plots were rewetted with an isotopically

enriched nutrient solution (^{15}N 1 atom%; 500 mL) of either nitrite (NO_2^- ; 1.3 mg $\text{NO}_2^- \cdot \text{N}^{-1}$; $n = 4$) as KNO_2 , nitrate (NO_3^- ; 3.5 mg $\text{NO}_3^- \cdot \text{N}^{-1}$; $n = 4$) as KNO_3 , or ammonium (NH_4^+ ; 9 mg $\text{NH}_4^+ \cdot \text{N}^{-1}$; $n = 4$) as NH_4Cl . The added N was expected to roughly double the background N content of soils to $1.2 \mu\text{g NO}_2^- \cdot \text{N g}^{-1}$, $3 \mu\text{g NO}_3^- \cdot \text{N g}^{-1}$, and $8 \mu\text{g NH}_4^+ \cdot \text{N g}^{-1}$, assuming a soil porosity of 54% ($1 - \rho_b/\rho_s$), such that the wetting front would penetrate roughly 3 cm, wetting ~ 1 kg of soil.

Unwetted chambers (ambient), used to describe prewetting conditions, were closed for 2 d and equipped with two NO_x pads (Ogawa & Co.) to capture NO for isotopic analysis. NO_x pads are routinely used in synoptic studies monitoring air pollution (62), and similar passive samplers have been used to measure $[\delta\text{-}^{15}\text{N}]\text{HNO}_3$ and $[\delta\text{-}^{18}\text{O}]\text{HNO}_3$ (63). As done with ambient chambers, control and isotopically labeled chambers were also equipped with two NO_x pads, but these pads were harvested at different time periods. The first set of pads were deployed from 0 to 15 min postwetting and were used to capture the wetting period, where NO emissions increase within seconds after rewetting soils. Another set of pads was deployed 15–60 min postwetting and was used to capture conditions leading to the “peak” in NO emissions during a NO pulse. A third and fourth set of pads were deployed 60 min to 1 d, and 1 d to 2 d postwetting, capturing the trail-off period when NO emissions decrease from peak to prewetting conditions. Complementary to soil chamber measurements, we also measured the isotopic composition of NO above the ground surface (denoted “atmospheric”) by deploying 8 NO_x pads ~ 3 m above the ground for 4 d.

The NO captured in the pads was measured as NO_2^- and analyzed for $[\delta\text{-}^{18}\text{O}]\text{NO}$ and $[\delta\text{-}^{15}\text{N}]\text{NO}$ using the bacterial denitrifier method (64) at the Facility for Isotope Ratio Mass Spectrometry (FIRMS) at the University of California, Riverside. During isotopic analyses, *Pseudomonas aureofaciens* was used for determining $[\delta\text{-}^{18}\text{O}]\text{NO}$ and $[\delta\text{-}^{15}\text{N}]\text{NO}$ in all samples. $\delta\text{-}^{15}\text{N}$ and $\delta\text{-}^{18}\text{O}$ values were measured using a Thermo Delta V isotope ratio mass spectrometer (Thermo Fisher Scientific) and the Gas Bench interface. The international reference materials United States Geological Survey (USGS)-32, USGS-34, and USGS-35 were included in each analytical run.

Because the NO_x pads can also adsorb nitrogen dioxide (NO_2), we tested for potential NO_2 contamination using the LMA-3 NO_2 analyzer and NO_2 pads. Both tests were negative for NO_2 , suggesting mostly NO was adsorbed by the NO_x pads. NO_x pads were stored in air-tight containers before and after field deployment. In the laboratory, harvested pads were extracted in 8 mL of DIW and placed in a wrist-action shaker overnight before isotopic analyses.

Based on the rapid transformation of $[\text{}^{15}\text{N}]\text{NO}_3^-$ to NO (Fig. 4), we evaluated whether the signal could have been attributable to $[\text{}^{15}\text{N}]\text{NO}_2^-$ contamination of the $[\text{}^{15}\text{N}]\text{NO}_3^-$ tracer. The $[\text{}^{15}\text{N}]\text{NO}_3^-$ tracer contained 0.003 mg of $\text{NO}_2^- \cdot \text{N L}^{-1}$, suggesting the NO_2^- would have had to be enriched by at least 7 atom% ^{15}N to explain the observed patterns (assuming a $0.6 \mu\text{g N g}^{-1}$ native soil NO_2^- pool and that the tracer infiltrated ~ 3 cm, wetting ~ 1 kg of soil). Although this level of contamination is possible, it is inconsistent with the patterns observed when we added 1 atom% $[\text{}^{15}\text{N}]\text{NO}_2^-$ to dry soils; the $[\text{}^{15}\text{N}]\text{NO}_2^-$ was rapidly consumed, peaking within 15 min postwetting, not after 15–60 min, as observed with the $[\text{}^{15}\text{N}]\text{NO}_3^-$ tracer (Fig. 4A). Moreover, the relatively small NO_2^- contamination is consistent with the background NO_2^- concentration in the KNO_3^- used to make the 1 atom% $[\text{}^{15}\text{N}]\text{NO}_3^-$ solution, suggesting that the NO_2^- contaminant was not isotopically enriched and that the rapid transformation of $[\text{}^{15}\text{N}]\text{NO}_3^-$ to NO was real.

Soil Sampling. We sampled surface soils (0–10 cm; A horizon) using a 10-cm corer (5-cm diameter). In the laboratory, soils were homogenized, sieved (4 mm), and analyzed for total C and N, extractable NH_4^+ , NO_2^- , and NO_3^- , WEON, and total extractable N (measured as the sum of WEON + NH_4^+ + NO_2^- + NO_3^-). Total soil C and N were measured in finely ground subsamples on a Thermo Flash EA 1112

analyzer. NH_4^+ and NO_3^- concentrations were measured by extraction with 2 M KCl (65), whereas WEON and NO_2^- were measured by extracting soils in DIW; NO_2^- was extracted in DIW because 2 M KCl underestimates NO_2^- (66). Soil extracts were analyzed colorimetrically for NH_4^+ [SEAL method Environmental Protection Agency (EPA)-126-A], NO_3^- (SEAL method EPA-129-A), and NO_2^- (SEAL method EPA-137-A) using a SEAL AQ-2 discrete analyzer. For the analysis of NO_2^- , we substituted ethylenediaminetetraacetic acid with diethylenetriaminepentaacetic acid to minimize interferences produced by iron (67). Water extracts for WEON were analyzed on a total organic carbon analyzer (TOC-V CSN; Shimadzu Scientific Instruments) using combustion catalytic oxidation/nondispersive infrared method with an ASI-V autosampler and TNM-1 total nitrogen module.

We measured rates of soil net N mineralization and nitrification in Ambient and No dry season plots, with and without plants, using a modified intact soil core technique (68). In November 2013, we collected 12 sets (four treatments \times three blocks) of duplicate cores (10-cm depth; 4-cm diameter) from the sampled treatments (three duplicate cores per treatment). Gravimetric soil moisture (oven-drying at 104°C for 24 h) and initial (T_0) exchangeable NH_4^+ and NO_3^- concentrations were determined on one set of cores. The remaining cores were capped with vented PVC covers to allow for gas exchange while preventing the inflow of water, returned to the plots, and incubated in their original holes for 4 wk to represent the early wet season. Rates of net N mineralization and nitrification were also measured in February (representing winter), April (representing spring), July (representing the early dry season), and October 2014 (representing the late dry season). Extracts were analyzed for NO_3^- and NH_4^+ as described above for soil analyses. Net N mineralization was calculated by subtracting total N at T_0 (exchangeable N) from total N at the end of the incubation (T_1) for each sampling date. Net nitrification was calculated by subtracting NO_3^- measured at T_0 from T_1 .

Soil WFPS (upper 10 cm) was measured on a monthly basis at each of the 48 plots using a portable MiniTrase Time Domain Reflectometer and Eq. 1 (Fig. S3B). A continuous record of soil moisture and temperature was obtained from the nearby Lisque weather station (2.6 km northwest of our site; 34.72449 N, 120.0635 W; 430 m ASL) operated by the Geography Department at the University of California, Santa Barbara (UC Santa Barbara) (Fig. S3A).

Statistical Analyses. We used a factorial-randomized complete block design with repeated-measures ANOVA and Tukey post hoc tests to detect significant effects of vegetation and dry season length on soil NO emissions and N concentrations (SAS software; SAS Institute). Our statistical analyses included all 48 plots, and although $n = 3$ for each treatment combination, the overall effect of vegetation of dry season length was assessed using 12 replicates. For example, the effect of removing all plants was replicated three times across four levels of dry season length. Differences in NO emissions between the dry and wet seasons were assessed in Ambient plots using a two-sample t test. When necessary, data were log-transformed to meet the assumption of normality. Statistical tests were considered significant when $P < 0.05$.

ACKNOWLEDGMENTS. We thank Eddie Dominguez, Matt Kamiyama, and Krystal Vasquez for help during soil laboratory analyses and gas flux calculations, as well as members of the J.P.S. laboratory for assistance in the field and for their insightful comments. We thank the Treseder lab at UC, Peter M. Vitousek, Steven D. Allison, and Eric A. Davidson, and an anonymous reviewer for their constructive criticism and Diane Alexander, Mark Fenn, and Andrzej Bytnerowicz from the US Forest Service for technical and logistical support. We also thank Kate McCurdy and the Sedgwick staff for assistance maintaining and accessing our research site. This research was funded by the National Science Foundation [postdoctoral fellowship to P.M.H. (DBI-1202894), DEB-1145875, and DEB-0614207] and the University of California, Riverside.

- Crutzen PJ (1979) Role of NO and NO_2 in the chemistry of the troposphere and stratosphere. *Annu Rev Earth Planet Sci* 7:443–472.
- Pilegaard K (2013) Processes regulating nitric oxide emissions from soils. *Philos Trans R Soc Lond B Biol Sci* 368(1621):20130126.
- Davidson EA, Kinglerlee W (1997) A global inventory of nitric oxide emissions from soils. *Nutr Cycl Agroecosyst* 48(1–2):37–50.
- Reynolds JF, et al. (2007) Global desertification: Building a science for dryland development. *Science* 316(5826):847–851.
- Feng S, Fu Q (2013) Expansion of global drylands under a warming climate. *Atmos Chem Phys* 13(19):10081–10094.
- Gao XJ, Giorgi F (2008) Increased aridity in the Mediterranean region under greenhouse gas forcing estimated from high resolution simulations with a regional climate model. *Global Planet Change* 62(3–4):195–209.
- Vourlitis GL, DeFotis C, Kristan W (2015) Effects of soil water content, temperature and experimental nitrogen deposition on nitric oxide (NO) efflux from semiarid shrubland soil. *J Arid Environ* 117:67–74.
- Delgado-Baquerizo M, et al. (2013) Aridity modulates N availability in arid and semiarid Mediterranean grasslands. *PLoS One* 8(4):e59807.
- Medinets S, Skiba U, Rennenberg H, Butterbach-Bahl K (2015) A review of soil NO transformation: Associated processes and possible physiological significance on organisms. *Soil Biol Biochem* 80:92–117.
- Donaldson MA, Bish DL, Raff JD (2014) Soil surface acidity plays a determining role in the atmospheric-terrestrial exchange of nitrous acid. *Proc Natl Acad Sci USA* 111(52):18472–18477.
- Heil J, Vereecken H, Bruggemann N (2016) A review of chemical reactions of nitrification intermediates and their role in nitrogen cycling and nitrogen trace gas formation in soil. *Eur J Soil Sci* 67(1):23–39.
- Russow R, Stange CF, Neue HU (2009) Role of nitrite and nitric oxide in the processes of nitrification and denitrification in soil: Results from N-15 tracer experiments. *Soil Biol Biochem* 41(4):785–795.
- Firestone MK, Davidson EA (1989) Microbial basis of NO and N_2O production and consumption in soil. *Exchange of Trace Gases Between Terrestrial Ecosystems and*

- the Atmosphere, eds Andreae MO, Schimel DS (John Wiley & Sons, New York), pp 7–21.
14. Schimel JP, Holland EA (2005) Global gases. *Principles and Applications of Soil Microbiology*, eds Sylvia DM, Fuhrmann JJ, Hartel PG, Zuberer DA (Prentice Hall, Upper Saddle River, NJ), 2nd Ed.
 15. Oswald R, et al. (2013) HONO emissions from soil bacteria as a major source of atmospheric reactive nitrogen. *Science* 341(6151):1233–1235.
 16. Skopp J, Jawsom MD, Doran JW (1990) Steady-state aerobic microbial activity as a function of soil water content. *Soil Sci Soc Am J* 54(6):1619–1625.
 17. Conrad R (1996) Soil microorganisms as controllers of atmospheric trace gases (H₂, CO, CH₄, OCS, N₂O, and NO). *Microbiol Rev* 60(4):609–640.
 18. Homyak PM, Sickman JO (2014) Influence of soil moisture on the seasonality of nitric oxide emissions from chaparral soils, Sierra Nevada, California, USA. *J Arid Environ* 103:46–52.
 19. Cardenas L, Rondon A, Johansson C, Sanhueza E (1993) Effects of soil moisture, temperature, and inorganic nitrogen on nitric oxide emissions from acidic tropical savannah soils. *J Geophys Res* 98(D8):14783–14790.
 20. Harms TK, Grimm NB (2012) Responses of trace gases to hydrologic pulses in desert floodplains. *J Geophys Res Biogeosci* 117(G1):G01035.
 21. Schimel JP, Bennett J (2004) Nitrogen mineralization: Challenges of a changing paradigm. *Ecology* 85(3):591–602.
 22. Hu S, Chapin FS, 3rd, Firestone MK, Field CB, Chiariello NR (2001) Nitrogen limitation of microbial decomposition in a grassland under elevated CO₂. *Nature* 409(6817):188–191.
 23. Davidson EA, et al. (1993) Processes regulating soil emissions of NO and N₂O in a seasonally dry tropical forest. *Ecology* 74(1):130–139.
 24. McCalley CK, Sparks JP (2009) Abiotic gas formation drives nitrogen loss from a desert ecosystem. *Science* 326(5954):837–840.
 25. Hall SJ, Huber D, Grimm NB (2008) Soil N₂O and NO emissions from an arid, urban ecosystem. *J Geophys Res Biogeosci* 113(G1):G01016.
 26. Homyak PM, et al. (2014) Assessing N saturation in a seasonally dry chaparral watershed: Limitations of traditional indicators of N saturation. *Ecosystems (N Y)* 17(7):1286–1305.
 27. Evans SE, Burke IC (2013) Carbon and nitrogen decoupling under an 11-year drought in the shortgrass steppe. *Ecosystems (N Y)* 16(1):20–33.
 28. Casciotti KL, Böhlke JK, McIlvin MR, Mroczkowski SJ, Hannon JE (2007) Oxygen isotopes in nitrite: Analysis, calibration, and equilibration. *Anal Chem* 79(6):2427–2436.
 29. Davidson EA (1992) Sources of nitric oxide and nitrous oxide following wetting of dry soil. *Soil Sci Soc Am J* 56(1):95–102.
 30. Venterea RT, Rolston DE, Cardon ZG (2005) Effects of soil moisture, physical, and chemical characteristics on abiotic nitric oxide production. *Nutr Cycl Agroecosyst* 72(1):27–40.
 31. Li XY, et al. (2006) Decadal-scale dynamics of water, carbon and nitrogen in a California chaparral ecosystem: DAYCENT modeling results. *Biogeochemistry* 77(2):217–245.
 32. Parker SS, Schimel JP (2011) Soil nitrogen availability and transformations differ between the summer and the growing season in a California grassland. *Appl Soil Ecol* 48(2):185–192.
 33. Pilegaard K, et al. (2006) Factors controlling regional differences in forest soil emission of nitrogen oxides (NO and N₂O). *Biogeochemistry* 3(4):651–661.
 34. Meixner T, Fenn M (2004) Biogeochemical budgets in a Mediterranean catchment with high rates of atmospheric N deposition - Importance of scale and temporal asynchrony. *Biogeochemistry* 70(3):331–356.
 35. Stark JM, Firestone MK (1995) Mechanisms for soil moisture effects on activity of nitrifying bacteria. *Appl Environ Microbiol* 61(1):218–221.
 36. Sullivan BW, Selman PC, Hart SC (2012) New evidence that high potential nitrification rates occur in soils during dry seasons: Are microbial communities metabolically active during dry seasons? *Soil Biol Biochem* 53:28–31.
 37. Gelfand I, Yakir D (2008) Influence of nitrite accumulation in association with seasonal patterns and mineralization of soil nitrogen in a semi-arid pine forest. *Soil Biol Biochem* 40(2):415–424.
 38. Su H, et al. (2011) Soil nitrite as a source of atmospheric HONO and OH radicals. *Science* 333(6049):1616–1618.
 39. Nelson DW, Bremner JM (1970) Role of soil minerals and metallic cations in nitrite decomposition and chemodenitrification. *Soil Biol Biochem* 2(1):1–8.
 40. Placella SA, Firestone MK (2013) Transcriptional response of nitrifying communities to wetting of dry soil. *Appl Environ Microbiol* 79(10):3294–3302.
 41. Blazewicz SJ, Schwartz E, Firestone MK (2014) Growth and death of bacteria and fungi underlie rainfall-induced carbon dioxide pulses from seasonally dried soil. *Ecology* 95(5):1162–1172.
 42. Tappe W, et al. (1999) Maintenance energy demand and starvation recovery dynamics of *Nitrosomonas europaea* and *Nitrobacter winogradskyi* cultivated in a retentostat with complete biomass retention. *Appl Environ Microbiol* 65(6):2471–2477.
 43. Kendall C, Caldwell EA (1998) Fundamentals of isotope geochemistry. *Isotope Tracers in Catchment Hydrology*, eds Kendall C, McDonnell JJ (Elsevier, Amsterdam), pp 51–86.
 44. Miller AE, Schimel JP, Meixner T, Sickman JO, Melack JM (2005) Episodic rewetting enhances carbon and nitrogen release from chaparral soils. *Soil Biol Biochem* 37(12):2195–2204.
 45. Robinson D (2001) δ¹⁵N as an integrator of the nitrogen cycle. *Trends Ecol Evol* 16(3):153–162.
 46. Davidson EA (1992) Pulses of nitric oxide and nitrous oxide flux following wetting of dry soil: An assessment of probable sources and importance relative to annual fluxes. *Ecol Bull* 42:149–155.
 47. Andersson KK, Hooper AB (1983) O₂ and H₂O are each the source of one O in NO₂ produced from NH₃ by *Nitrosomonas*: ¹⁵N-NMR evidence. *FEBS Lett* 164(2):236–240.
 48. Buchwald C, Santoro AE, McIlvin MR, Casciotti KL (2012) Oxygen isotopic composition of nitrate and nitrite produced by nitrifying cocultures and natural marine assemblages. *Limnol Oceanogr* 57(5):1361–1375.
 49. Beaumont HJE, Lens SI, Westerhoff HV, van Spanning RJA (2005) Novel nirK cluster genes in *Nitrosomonas europaea* are required for NirK-dependent tolerance to nitrite. *J Bacteriol* 187(19):6849–6851.
 50. Austin AT, Vitousek PM (1998) Nutrient dynamics on a precipitation gradient in Hawai'i. *Oecologia* 113(4):519–529.
 51. Wang C, et al. (2014) Aridity threshold in controlling ecosystem nitrogen cycling in arid and semi-arid grasslands. *Nat Commun* 5:4799.
 52. Delgado-Baquerizo M, et al. (2013) Decoupling of soil nutrient cycles as a function of aridity in global drylands. *Nature* 502(7473):672–676.
 53. Pardo LH, Hemond HF, Montoya JP, Fahey TJ, Siccama TG (2002) Response of the natural abundance of N-15 in forest soils and foliage to high nitrate loss following clear-cutting. *Can J For Res* 32(7):1126–1136.
 54. Jenny H (1941) *Factors of Soil Formation: A System of Quantitative Pedology* (McGraw-Hill, New York).
 55. Vitousek PM, Porder S, Houlton BZ, Chadwick OA (2010) Terrestrial phosphorus limitation: Mechanisms, implications, and nitrogen-phosphorus interactions. *Ecol Appl* 20(1):5–15.
 56. Fenn ME, et al. (2010) Nitrogen critical loads and management alternatives for N-impacted ecosystems in California. *J Environ Manage* 91(12):2404–2423.
 57. Fierer N, Chadwick OA, Trumbore SE (2005) Production of CO₂ in soil profiles of a California annual grassland. *Ecosystems (N Y)* 8(4):412–429.
 58. Davidson EA, et al. (1991) Soil emissions of nitric oxide in a seasonally dry tropical forest of Mexico. *J Geophys Res* 96(D8):15439–15445.
 59. Hutchinson GL, Yang WX, Andre CE (1999) Overcoming humidity dependence of the chromium trioxide converter used in luminol-based nitric oxide detection. *Atmos Environ* 33(1):141–145.
 60. Kelly TJ, Spicer CW, Ward GF (1990) An assessment of the luminol chemiluminescence technique for measurement of NO₂ in ambient air. *Atmos Environ A Gen Topics* 24(9):2397–2403.
 61. US Environmental Protection Agency (2015) National Trends in Nitrogen Dioxide and Ozone Levels (US Environmental Protection Agency, Washington, DC), Updated February 23, 2016. Available at <https://www3.epa.gov/airtrends/index.html>. Accessed February 23, 2016.
 62. DeForest Hauser C, Buckley A, Porter J (2015) Passive samplers and community science in regional air quality measurement, education and communication. *Environ Pollut* 203:243–249.
 63. Bell MD, Sickman JO, Bytnerowicz A, Padgett PE, Allen EB (2014) Variation in isotopologues of atmospheric nitric acid in passively collected samples along an air pollution gradient in southern California. *Atmos Environ* 94:287–296.
 64. Sigman DM, et al. (2001) A bacterial method for the nitrogen isotopic analysis of nitrate in seawater and freshwater. *Anal Chem* 73(17):4145–4153.
 65. Maynard DG, Kalra YP, Crumbaugh JA (2007) Nitrate and exchangeable ammonium nitrogen. *Soil Sampling and Methods of Analysis*, eds Carter MR, Gregorich EG (CRC Press, Boca Raton, FL), 2nd Ed, pp 71–80.
 66. Homyak PM, Vasquez KT, Sickman JO, Parker DR, Schimel JP (2015) Improving nitrite analysis in soils: Drawbacks of the conventional 2 M KCl extraction. *Soil Sci Soc Am J* 79(4):1237–1242.
 67. Colman BP, Schimel JP (2010) Understanding and eliminating iron interference in colorimetric nitrate and nitrite analysis. *Environ Monit Assess* 165(1-4):633–641.
 68. DiStefano JF, Gholz JL (1986) A proposed use of ion exchange resin to measure nitrogen mineralization and nitrification in intact soil cores. *Commun Soil Sci Plant Anal* 17(9):989–998.

Supporting Information

Homyak et al. 10.1073/pnas.1520496113

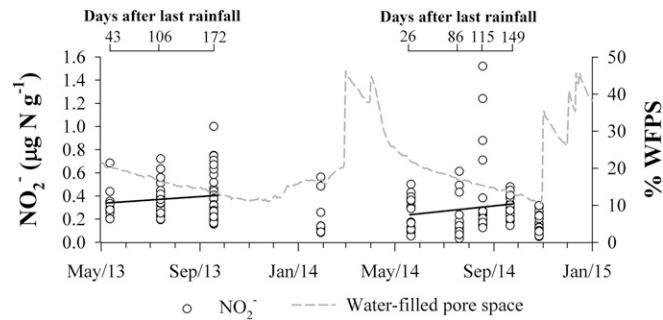


Fig. S1. Soil nitrite concentrations from Ambient and Extended dry season plots as a function of soil WFPS and number of days since the last rainfall event. The relationship between soil NO_2^- concentrations and the number of days after the last rainfall was positive but not significant ($P = 0.6$ in 2013 and $P = 0.3$ in 2014).

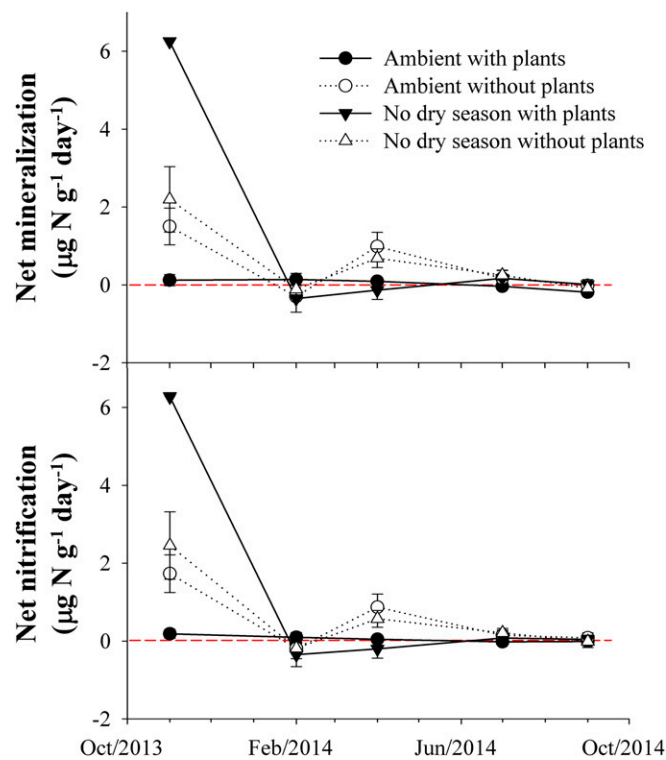


Fig. S2. Average (\pm SEM; $n = 3$) rates of net N mineralization and nitrification in Ambient and No dry season plots with and without plants. During November 2013, two of the three cores were destroyed by wildlife and were not included in the analysis ($n = 1$).

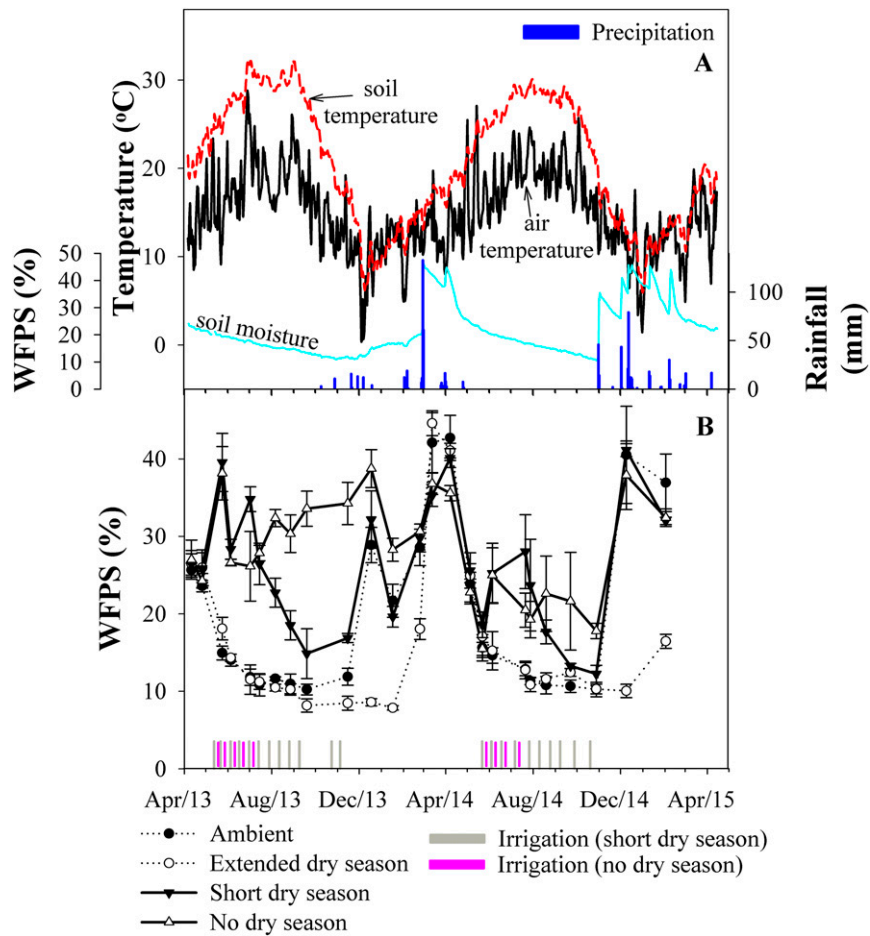


Fig. S3. Climatic variables measured at the Lisque weather station operated by UC Santa Barbara (A) and average (\pm SEM; $n = 3$) soil WFPS measured at a 10-cm depth in plots with plants across the dry season length manipulation treatments (B). Extended dry season rainout shelters were removed on January 30, 2014 for WY 2013 and January 19, 2015 for WY 2014. Irrigation periods are represented by bars across the x axis, where duplicate bars represent watering of both the Short dry season and No dry season treatments.